Mineralogical Magazine, June 2015, Vol. 79(3), pp. 767–780

Waimirite-(Y), orthorhombic YF_3, a new mineral from the Pitinga mine, Presidente Figueiredo, Amazonas, Brazil and from Jabal Tawlah, Saudi Arabia: description and crystal structure

Daniel Atencio[1,*], Artur C. Bastos Neto[2], Vitor P. Pereira[2], José T. M. M. Ferron[3], M. Hoshino[4], T. Moriyama[4], Y. Watanabe[4], R. Miyawaki[5], José M. V. Coutinho[1], Marcelo B. Andrade[6], Kenneth Domanik[7], Nikita V. Chukanov[8], K. Momma[5], H. Hirano[4] and M. Tsunematsu[4]

[1] Instituto de Geociências, Universidade de São Paulo, Rua do Lago 562, 05508-080, São Paulo, SP, Brazil
[2] Instituto de Geociências, Universidade Federal do Rio Grande do Sul. Avenida Bento Gonçalves 9500, CEP 91501-970, Porto Alegre, RS, Brazil
[3] Programa de Pós-graduação em Geociências, Instituto de Geociências, Universidade Federal do Rio Grande do Sul, Brazil
[4] Institute for Geo-Resources and Environment, National Institute of Advanced Industrial Science and Technology, Central 7, 1-1-1 Higashi, Tsukuba, Ibaraki 305-8567, Japan
[5] Department of Geology and Paleontology, National Museum of Nature and Science, 4-1-1 Amakubo, Tsukuba, Ibaraki 305-0005, Japan
[6] São Carlos Institute of Physics, University of São Paulo, Caixa Postal 369, 13560-970, São Carlos, SP, Brazil
[7] Lunar and Planetary Laboratory, University of Arizona, 1629 E. University Blvd., Tucson, AZ, 85721-0092, USA
[8] Institute of Problems of Chemical Physics, Russian Academy of Sciences, Chernogolovka, Moscow region, 142432 Russia

[*Received 12 August 2014; Accepted 8 January 2015; Associate Editor: D. Hibbs*]

ABSTRACT

Waimirite-(Y) (IMA 2013-108), orthorhombic YF_3, occurs associated with halloysite, in hydrothermal veins (up to 30 mm thick) cross-cutting the albite-enriched facies of the A-type Madeira granite (~1820 Ma), at the Pitinga mine, Presidente Figueiredo Co., Amazonas State, Brazil. Minerals in the granite are 'K-feldspar', albite, quartz, riebeckite, 'biotite', muscovite, cryolite, zircon, polylithionite, cassiterite, pyrochlore-group minerals, 'columbite', thorite, native lead, hematite, galena, fluorite, xenotime-(Y), gagarinite-(Y), fluocerite-(Ce), genthelvite–helvite, topaz, 'illite', kaolinite and 'chlorite'. The mineral occurs as massive aggregates of platy crystals up to ~1 μm in size. Forms are not determined, but synthetic YF_3 displays pinacoids, prisms and bipyramids. Colour: pale pink. Streak: white. Lustre: non-metallic. Transparent to translucent. Density (calc.) = 5.586 g/cm^3 using the empirical formula. Waimirite-(Y) is biaxial, mean n = 1.54–1.56. The chemical composition is (average of 24 wavelength dispersive spectroscopy mode electron microprobe analyses, O calculated for charge balance): F 29.27, Ca 0.83, Y 37.25, La 0.19, Ce 0.30, Pr 0.15, Nd 0.65, Sm 0.74, Gd 1.86, Tb 0.78, Dy 8.06, Ho 1.85, Er 6.38, Tm 1.00, Yb 5.52, Lu 0.65, O (2.05), total (97.53) wt.%. The empirical formula (based on 1 cation) is $(Y_{0.69}Dy_{0.08}Er_{0.06}Yb_{0.05}Ca_{0.03}Gd_{0.02}Ho_{0.02}Nd_{0.01}Sm_{0.01}Tb_{0.01}Tm_{0.01}Lu_{0.01})_{\Sigma 1.00}[F_{2.54}\square_{0.25}O_{0.21}]_{\Sigma 3.00}$. Orthorhombic, *Pnma*, a = 6.386(1), b = 6.877(1), c = 4.401(1) Å, V = 193.28(7) Å^3, Z = 4 (powder data). Powder X-ray diffraction (XRD) data [d in Å (I) (hkl)]: 3.707 (26) (011), 3.623 (78) (101), 3.438 (99) (020), 3.205 (100) (111), 2.894 (59) (210), 1.937 (33) (131), 1.916 (24) (301), 1.862 (27) (230). The name

* E-mail: datencio@usp.br
DOI: 10.1180/minmag.2015.079.3.18

is for the Waimiri-Atroari Indian people of Roraima and Amazonas. A second occurrence of waimirite-(Y) is described from the hydrothermally altered quartz-rich microgranite at Jabal Tawlah, Saudi Arabia. Electron microprobe analyses gave the empirical formula $(Y_{0.79}Dy_{0.08}Er_{0.05}Gd_{0.03}Ho_{0.02}Tb_{0.01}Tm_{0.01}Yb_{0.01})_{\Sigma 1.00}[F_{2.85}O_{0.08}\square_{0.07}]_{\Sigma 3.00}$. The crystal structure was determined with a single crystal from Saudi Arabia. Unit-cell parameters refined from single-crystal XRD data are a = 6.38270(12), b = 6.86727(12), c = 4.39168(8) Å, V = 192.495(6) Å^3, Z = 4. The refinement converged to R_1 = 0.0173 and wR_2 = 0.0388 for 193 independent reflections. Waimirite-(Y) is isomorphous with synthetic SmF_3, HoF_3 and YbF_3. The Y atom forms a 9-coordinated YF_9 tricapped trigonal prism in the crystal structure. The substitution of Y for Dy, as well as for other lanthanoids, causes no notable deviations in the crystallographic values, such as unit-cell parameters and interatomic distances, from those of pure YF_3.

Keywords: waimirite-(Y), new mineral, hydrothermal vein, yttrium fluoride, Pitinga mine, Presidente Figueiredo Co., Amazonas State, Brazil, Jabal Tawlah, Saudi Arabia.

Introduction

THE present paper describes a new mineral species waimirite-(Y), YF_3, from hydrothermal veins cross-cutting the albite-enriched granite facies at the Pitinga mine, Brazil. During the geological survey on the rare-earth element (*REE*) deposits in Saudi Arabia (Watanabe *et al*., 2014), a second occurrence of waimirite-(Y) in an ore body was noticed. Using some anhedral-to-subhedral crystals of waimirite-(Y) from Saudi Arabia, we have determined and refined the composition and crystal structure, respectively.

The distinct crystal structures between the orthorhombic YF_3, waimirite-(Y) and the trigonal CeF_3, fluocerite-(Ce), (Cheetham *et al*., 1976; Garashina *et al*., 1980; Zalkin and Templeton, 1985; Kondratyuk *et al*., 1988) demonstrate a difference in crystallographic feature for the fluorides of smaller and larger rare-earth ions, namely Y^{3+} and Ce^{3+}, respectively.

Synthetic YF_3 is known in two polymorphic forms: (α) trigonal, *P*3*m*1, stable from 1077ºC to 1162ºC, when it melts and (β) orthorhombic, *Pnma*, stable below 1077ºC. The "cubic YF_3" of Nowacki (1938) is in fact the phase NaY_3F_{10} (Zalkin and Templeton, 1953). Waimirite-(Y) (IMA 2013-108) is equivalent to the β phase. Single crystals of the latter have been prepared and used for the structure determination. Fluocerite-(Ce) and fluocerite-(La) are trigonal CeF_3 and LaF_3, respectively. As waimirite-(Y) has crystal-structure characteristics more closely related to those of high-Z *REE*F_3 phases than to those of their low-Z counterparts, a new root name was created.

The most interesting feature of the new mineral, from both the crystal-chemical and potential application aspects, is the distribution of *REE* (i.e. heavy, *HREE*; and light, *LREE*). In waimirite-(Y), the (*HREE*+Y)/*LREE* ratio is ~18 and the Y/*Ln* ratio, where *Ln* means lanthanides ^{57}La to ^{72}Lu, is ~2.5. Clearly it is a *HREE* mineral as is also the case for xenotime-(Y), where no more than 2% *LREE* occur. In xenotime-(Y) from Pitinga *LREE*s are virtually absent. Its unit cell is smaller than that of common xenotime-(Y), due to the substitution of O by F, forming PO_3F tetrahedra (Bastos Neto *et al*., 2013). Ideal *Ln*-free waimirite-(Y) contains 60.93 wt.% of yttrium, whereas the Y content in ideal xenotime-(Y) is 48.35 wt.%. Waimirite-(Y) could be, therefore, a spectacular ore mineral.

Rare-earth element fluoride crystalline materials are commonly studied owing to their applications in solid-state lasers and scintillators. Indeed, their good optical properties as well as their low non-radioactive emissions (mainly because of the low cut-off phonon frequencies) make these materials good host matrices for visible or infrared light emission and other optical applications. It is well known that fluoride materials can be used as active media for tunable solid-state lasers (Lage *et al*., 2004). The orthorhombic YF_3 crystals are non-hygroscopic and colourless under normal conditions, which is essential for their use as active laser materials. Kollia *et al.* (1995) showed that YF_3 could be a laser material.

Both the description and the name of the new mineral were approved by the Commission on New Minerals, Nomenclature and Classification of the International Mineralogical Association (IMA) (IMA 2013-108, Bastos Neto *et al*., 2014*b*). The name waimirite is for the Waimiri-Atroari Indian people of Roraima and Amazonas. The mine is located close to the Indian Territory. The suffix "(Y)" was introduced because it is a

https://doi.org/10.1180/minmag.2015.079.3.18 Published online by Cambridge University Press

rare-earth mineral. The name "waimirite" was used informally for this mineral by Minuzzi *et al*. (2003). The same authors applied the name "atroarite" for a probable ralstonite.

Type material has been deposited in the collections of the Museu de Geociências, Instituto de Geociências, Universidade de São Paulo, Rua do Lago, 562, 05508-080 - São Paulo, SP, Brazil, specimen number DR919 and in the Museu de Mineralogia Luiz Englert, Departamento de Mineralogia e Petrologia, Instituto de Geociências, Universidade Federal do Rio Grande do Sul, Avenida Bento Gonçalves 9500, 91501-970, Porto Alegre, RS, Brazil, specimen number 3620. Part of the cotype sample has been deposited at the University of Arizona Mineral Museum, RRUFF Project (http://rruff.info/R130714).

Occurrence

In the type locality, Pitinga mine (0º44′43″S 60º7′40″W), Presidente Figueiredo, Amazonas, Brazil (Bastos Neto *et al*., 2009, 2014*a*), waimirite-(Y) forms hydrothermal veins (up to 30 mm thick) cross-cutting the albite-enriched facies of A-type Madeira granite (~1820 Ma). The Madeira granite is hosted by A-type volcanic rocks (Iricoumé Group, ~1880 Ma) which formed in a caldera complex. The albite-enriched granite facies corresponds to the Madeira world-class Sn-Nb-Ta (*REE*, F, Zr, Li and Th) deposit, with 130 million tons of disseminated ore. In addition, in the central portion of the albite-enriched granite facies, there is a massive cryolite deposit of 10 million tons with a grade of 31.9% Na_3AlF_6. This association of Sn with several rare metals in the same albite-enriched granite that hosts a massive cryolite deposit is unique in the world. The directly associated mineral is halloysite. Minerals in the albite-enriched granite are quartz, 'K-feldspar', albite, riebeckite, 'biotite', muscovite, cryolite, zircon, polylithionite, cassiterite, pyrochlore-group minerals, 'columbite', thorite, lead, galena, fluorite, xenotime-(Y), gagarinite-(Y), fluocerite-(Ce), genthelvite-helvite, topaz, 'illite', kaolinite and 'chlorite'. At the magmatic stage, the high F content in the melt was buffered by crystallization of cryolite. Tin, Nb and *REE* were dispersed homogeneously throughout the deposit, transported by F-bearing complexes in the melt and concentrated in the forms of cassiterite, a U-Pb-rich pyrochlore-group mineral and xenotime-(Y), respectively. Zircon crystallization, inhibited at the early magmatic stage by high F activity, intensified at the late magmatic stage owing to a decrease in alkalinity associated with riebeckite crystallization, forming concentrations, together with xenotime and polythionite, in pegmatitic zones. Rare-earth element mineralization in the lower portion of the massive cryolite deposit is represented by gagarinite-(Y), with fluocerite-(Ce) inclusions formed by exsolution of the early gagarinite. There is no evidence for either silicate–fluoride liquid immiscibility or a continuous transition from volatile-rich silicate melt to solute-rich fluids. The abrupt magmatic–hydrothermal transition triggered three processes: (1) albitization accompanied by the crystallization of hydrothermal cryolite in the rock matrix; (2) conversion of pyrochlore to a columbite-group mineral, characterized by gradual loss of Pb and enrichment in U and Nb; and (3) formation of the massive cryolite deposit, comprised of crystals of twinned cryolite (87%) with subordinate quartz, 'K-feldspar' and zircon from an aqueous saline (1.7 to 22.4 wt.% equiv. NaCl) hydrothermal fluid, starting at a minimum temperature of 400ºC and continuing down-temperature. The evolution of parameters (*REE*, La/Lu, *LREE/HREE*, Y) in cryolite is continuous from the magmatic stage to the low-temperature hydrothermal stage.

Waimirite-(Y) also occurs as the main *REE* mineral in hydrothermally altered quartz-rich microgranite at Jabal Tawlah (Mount Tawlah) in the Kingdom of Saudi Arabia. It is present as inclusions in an undetermined Ca-Y-F mineral. Anhedral-to-subhedral crystals of several tens to

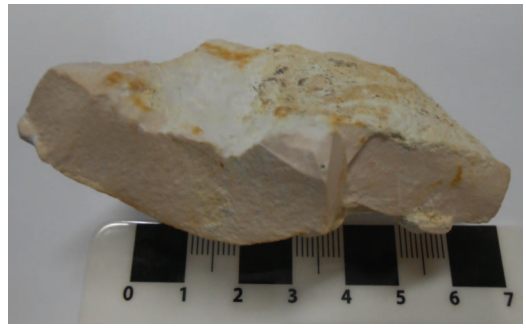

FIG. 1. Waimirite-(Y) bearing sample from the Pitinga mine, Presidente Figueiredo, Amazonas, Brazil. Cotype material (number DR919) deposited in the collections of the Museu de Geociências, USP, São Paulo, Brazil.

https://doi.org/10.1180/minmag.2015.079.3.18 Published online by Cambridge University Press

several hundreds of μm in size are common. Associated minerals are 'biotite', albite, muscovite, microcline, columbite-(Fe), zircon, thorite, xenotime-(Y), samarskite-(Y), ilmenite, an undetermined Ca-Y-F mineral, euxenite-(Y), fergusonite-(Y), rutile, 'illite', baryte, calcite and goethite. Waimirite-(Y) was formed from fluorine-rich hydrothermal fluids containing large amounts of *REE*.

Habit and physical properties

Waimirite-(Y) from Brazil occurs as aggregates of platy crystals up to ~1 μm (Figs 1 and 2).

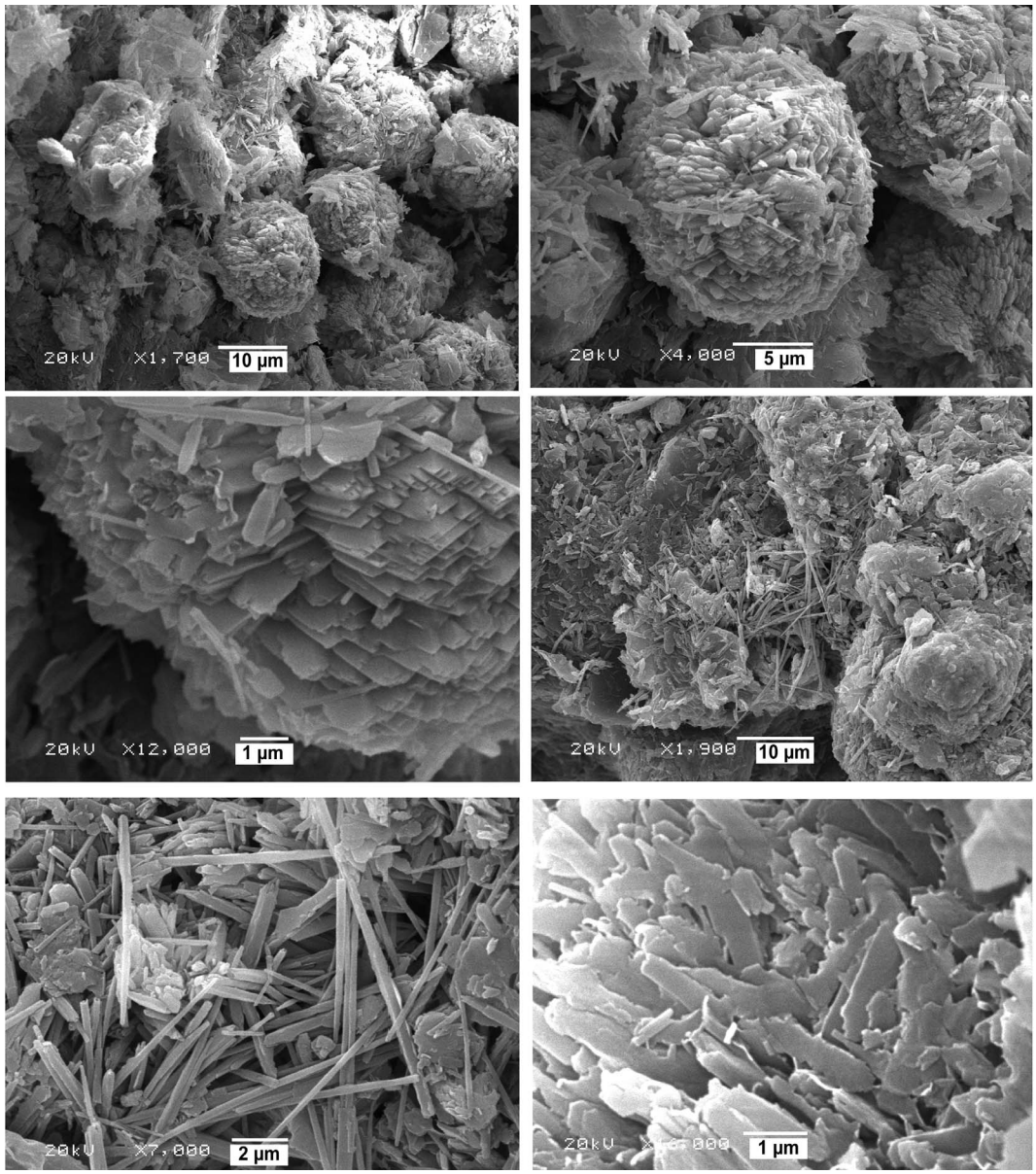

FIG. 2. Backscattered electron image of waimirite-(Y) from Brazil (spherical aggregates of plates) and halloysite (tubes).

https://doi.org/10.1180/minmag.2015.079.3.18 Published online by Cambridge University Press

Forms were not determined, but synthetic YF_3 displays pinacoids, prisms and bipyramids (Qian *et al*., 2010). Cleavage was not observed, but synthetic YF_3 displays perfect cleavage on {010} (Rotereau *et al*., 1993). Parting was not observed. The mineral is transparent to translucent under transmitted light microscopy and displays a non-metallic lustre; it is pale pink and the streak is white. It is non-fluorescent under long wavelength (365 nm) ultraviolet radiation. The Mohs hardness was not measured due to the small crystal sizes. Fracture was not determined. Density could not be measured due to the crystal dimensions. The density calculated from the empirical formula and refined unit-cell dimensions is 5.586 g/cm^3. Optically the mineral is biaxial; due to the crystal dimensions, only a mean n = 1.54–1.56 was measured.

Waimirite-(Y) from Saudi Arabia (Fig. 3) is colourless with a white streak. It is transparent and the lustre is vitreous. Cleavage is not observed and the fracture is irregular to conchoidal. The tenacity is brittle. The density could not be measured because of small grain sizes. The calculated density is 5.678 g/cm^3 on the basis of the empirical formula and refined unit-cell dimensions. The Vickers microhardness is 667–786 (mean 700) kg/mm^2 (100 g load), corresponding to 5½–6 on the Mohs scale. It is optically biaxial positive with 2V = 70–80º. The mean refractive index is estimated as 1.60, because it is higher than that of albite (1.57) and lower than that of apatite (1.64) in thin section.

Mineral chemistry

Waimirite-(Y) crystals from Brazil were embedded in epoxy resin and polished. Chemical analyses (24) were completed with a CAMECA SX-100 electron microprobe (wavelength dispersive spectroscopy (WDS) mode, 15 kV, 20 nA, ~5 μm beam diameter) at the University of Arizona Electron Microprobe Laboratory. A preliminary WDS scan at high current showed no peak for Eu. This indicates that it is either not present or present at <~0.01 wt.%. The actual analyses were performed at a much lower current because the sample is very easily damaged under the electron beam. The three sigma detection limits under the conditions of the analyses range from ~0.07 to 0.13 wt.% for the *Ln* actually observed. The *REE* standards are synthetic glasses from the University of Edinburgh. Each glass has a single *REE*, present at a concentration of ~20 wt.% oxide, in a Si-Al-Ca-O based matrix. Analytical results are represented in Table 1. Silicon (0.12 wt.%) and Al (0.10 wt.%) were subtracted because they

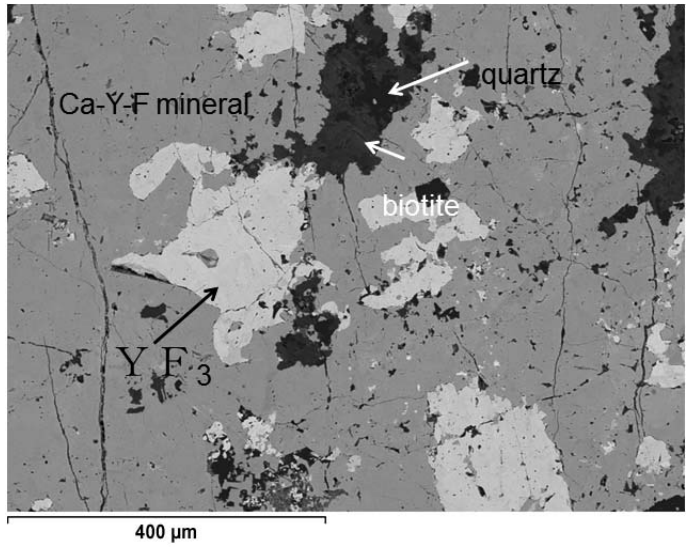

FIG. 3. Backscattered electron image of waimirite-(Y) from Saudi Arabia (light grey, subhedral crystal at the centre) associated with biotite (dark grey) and quartz (black) enclosed in the undetermined Ca-Y-F mineral (medium grey). Field of view: ~0.86 mm × 0.65 mm.

https://doi.org/10.1180/minmag.2015.079.3.18 Published online by Cambridge University Press

TABLE 1. Analytical data for waimirite-(Y) from Brazil (mean of 24 point analyses).

Constituent	Wt.%	Range	SD	Probe standard
F	29.27	28.43–30.19	0.47	MgF_2
Y	37.25	34.78–38.89	1.16	YAG
La	0.19	0.01–0.28	0.06	La_Ed
Ce	0.30	0.19–0.46	0.07	Ce_Ed
Pr	0.15	0.03–0.25	0.08	Pr_Ed
Nd	0.65	0.57–0.81	0.06	Nd_Ed
Sm	0.74	0.66–0.87	0.05	Sm_Ed
Gd	1.86	1.65–2.09	0.11	Gd_Ed
Tb	0.78	0.60–0.95	0.08	Tb_Ed
Dy	8.06	7.36–8.81	0.34	Dy_Ed
Ho	1.85	1.47–2.35	0.23	Ho_Ed
Er	6.38	5.80–7.24	0.36	Er_Ed
Tm	1.00	0.69–1.34	0.17	Tm_Ed
Yb	5.52	4.99–6.16	0.26	Yb_Ed
Lu	0.65	0.38–1.58	0.24	Lu_Ed
Ca	0.83	0.71–0.97	0.07	diopside
O	(2.05)			
Total	(97.53)			

belong to the associated halloysite. The percentage of F obtained from the chemical analysis of waimirite-(Y) is not sufficient to neutralize the cations. The presence of O is required. If we consider O = 2.05 wt.%, the formula is charge-balanced. The empirical formula (based on

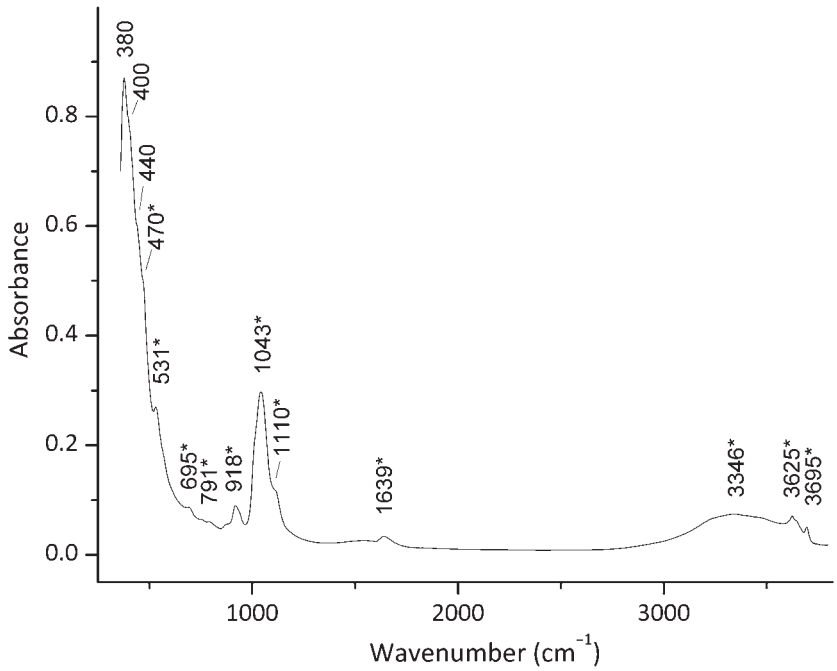

FIG. 4. Infrared spectrum of waimirite-(Y) with halloysite admixture (the bands marked with *) from Brazil.

https://doi.org/10.1180/minmag.2015.079.3.18 Published online by Cambridge University Press

TABLE 2. Analytical data for waimirite-(Y) from Saudi Arabia (mean of 24 point analyses).

Constituent	Wt.%	Range	SD	Probe standard
F	34.34	33.44–35.19	0.88	DyF_3
Y	44.61	43.22–48.84	1.32	Y-Glass: SiO_2 54.3, Al_2O_3 12.7, CaO 20.5, Y_2O_3 11.8 wt.%
Ce	0.08	0.04–0.12	0.04	Ce-Glass: SiO_2 54.2, Al_2O_3 12.8, CaO 20.4, Ce_2O_3 11.9 wt.%
Nd	0.04	0.02–0.07	0.03	Nd-Glass: SiO_2 54.4, Al_2O_3 12.8, CaO 20.6, Nd_2O_3 11.8 wt.%
Sm	0.14	0.11–0.18	0.03	Sm-Glass: SiO_2 54.7, Al_2O_3 12.9, CaO 20.8, Sm_2O_3 11.2 wt.%
Gd	2.95	2.57–3.41	0.43	Gd-Glass: SiO_2 54.8, Al_2O_3 12.1, CaO 20.7, Gd_2O_3 12.1 wt.%
Tb	0.72	0.59–0.81	0.12	Tb-Glass: SiO_2 54.6, Al_2O_3 12.6, CaO 20.2, Tb_2O_3 11.9 wt.%
Dy	7.77	6.84–7.96	0.86	Dy-Glass: SiO_2 54.7, Al_2O_3 12.5, CaO 20.6, Dy_2O_3 12.0 wt.%
Ho	2.27	1.95–2.50	0.29	Ho-Glass: SiO_2 54.6, Al_2O_3 12.8, CaO 20.7, Ho_2O_3 11.9 wt.%
Er	5.39	5.05–5.68	0.32	Er-Glass: SiO_2 54.6, Al_2O_3 12.6, CaO 20.5, Er_2O_3 11.9 wt.%
Tm	0.69	0.61–0.75	0.07	Tm-Glass: SiO_2 54.8, Al_2O_3 12.4, CaO 20.3, Tm_2O_3 11.9 wt.%
Yb	1.36	1.03–1.56	0.29	Yb-Glass: SiO_2 54.7, Al_2O_3 12.6, CaO 20.7, Yb_2O_3 1.02 wt.%
Na	0.06	0.02–0.09	0.04	$NaAlSi_3O_8$
Ca	0.08	0.03–0.05	0.02	$CaSiO_3$
O	(0.80)			
Total	(101.30)			

one cation) is $(Y_{0.69}Dy_{0.08}Er_{0.06}Yb_{0.05}Ca_{0.03}Gd_{0.02}Ho_{0.02}Nd_{0.01}Sm_{0.01}Tb_{0.01}Tm_{0.01}Lu_{0.01})_{\Sigma 1.00}[F_{2.54}O_{0.21}\square_{0.25}]_{\Sigma 3.00}$. The low analytical total is assumed to be due to the subtraction of halloysite. Note that ionic conductivity of synthetic orthorhombic YF_3 and HoF_3 is related to vacancies in F sites (Sorokin *et al*., 2002, Trnovcová *et al*., 2003). Vacancy abundance in the study of synthetic HoF_3 (Sorokin *et al*., 2002) is comparable with values inferred for waimirite-(Y). The simplified formula YF_3 requires: Y 60.93, F 39.07, total 100.00 wt.%.

Chemical analyses for waimirite-(Y) from Saudi Arabia were carried out with a JEOL

TABLE 3. Powder XRD data for waimirite-(Y).

			1			2		3	
h	*k*	*l*	$d_{calc.}$ (Å)	$d_{obs.}$ (Å)	$I_{obs.}$	$d_{obs.}$ (Å)	$I_{obs.}$	$d_{obs.}$ (Å)	$I_{obs.}$
0	1	1	**3.707**	**3.707**	**26**	3.70	28	3.696	55
1	0	1	**3.624**	**3.623**	**78**	3.62	49	3.612	75
0	2	0	**3.439**	**3.438**	**99**	3.43	55	3.426	75
1	1	1	**3.206**	**3.205**	**100**	3.20	100	3.197	100
2	1	0	**2.896**	**2.894**	**59**	2.90	71	2.886	95
2	0	1	2.584	2.587	4			2.577	5
1	2	1	2.494	2.495	17	2.49	20	2.488	50
2	1	1	2.419	2.420	6	2.42	4	2.413	25
2	2	0	2.340	2.340	4	2.34	6	2.332	19
0	0	2	2.200	2.203	10	2.20	16	2.196	45
1	0	2	2.080					2.076	2
2	2	1	2.066	2.067	19	2.07	24	2.060	80
0	3	1	2.033					2.027	1
1	1	2	1.991	1.993	14	1.988	30	1.987	85
1	3	1	**1.937**	**1.937**	**33**	1.935	55	1.932	100
3	0	1	**1.916**	**1.916**	**24**			1.910	95
2	3	0	**1.862**	**1.862**	**27**	1.859	40	1.856	100
0	2	2	1.853			1.848	32	1.849	60
3	1	1	1.846	1.845	17			1.840	70
1	2	2	1.780	1.780	8	1.777	25	1.776	70
2	1	2	1.752	1.752	11	1.749	12	1.748	70
0	4	0	1.719	1.719	10	1.717	11	1.714	60
3	2	1	1.674	1.674	10	1.672	17	1.669	70
4	0	0	1.596	1.597	4	1.596	11	1.591	35
1	4	1	1.553	1.553	5	1.551	8	1.549	35
1	3	2	1.541	1.538	4	1.538	6	1.537	25
3	0	2	1.530	1.524	4			1.526	7
2	4	0	1.514					1.509	1
4	0	1	1.501					1.496	5
3	1	2	1.493	1.494	4	1.491	4	1.490	35
4	1	1	1.466	1.467	5	1.467	12	1.466	45
4	2	0	1.448	1.447	3	1.447	10	1.443	25
0	1	3	1.435	1.432	3	1.431	14	1.432	25
2	4	1	1.431					1.427	20
2	3	2	1.421	1.424	4	1.419	10	1.418	50
1	1	3	1.400			1.397	5	1.397	12
3	2	2	1.398	1.399	3			1.394	15
4	2	1	1.375					1.371	4
0	4	2	1.355	1.355	3	1.354	11	1.351	25

1. Pitinga mine, Presidente Figueiredo, Amazonas, Brazil (this paper). The strongest lines are given in bold.
2. Jabal Tawlah, Saudi Arabia (this paper).
3. Synthetic (Greis, 1976); a = 6.3654, b = 6.8566, c = 4.3916 Å, V = 191.67 Å^3: PDF#32-1431.

https://doi.org/10.1180/minmag.2015.079.3.18 Published online by Cambridge University Press

JXA-8900 WDS electron microprobe analyser (20 kV, 20 nA, beam diameter = 2 μm). The average of five analyses and standard materials are presented in Table 2. The empirical formula is $(Y_{0.79}Dy_{0.08}Er_{0.05}Gd_{0.03}Ho_{0.02}Tb_{0.01}Tm_{0.01}Yb_{0.01})_{\Sigma 1.00}[F_{2.85}O_{0.08}\square_{0.07}]_{\Sigma 3.00}$ on the basis of one cation.

Infrared spectrometry

The infrared (IR) absorption spectrum of waimirite-(Y) (Fig. 4) was obtained from a powdered sample (mixed with KBr and pelletized) using a Bruker Alpha FTIR spectrometer in the range from 360 to 3800 cm^{-1}, with resolution of 4 cm^{-1}. A strong band at 380 cm^{-1} (with shoulders at 400 and 440 cm^{-1}) corresponds to waimirite-(Y). All bands marked by an asterisk correspond to H_2O-bearing halloysite and coincide with the bands in the IR spectrum of halloysite-10 Å (Chukanov, 2014). In particular, the bands at 1639 and 3346 cm^{-1} correspond to H_2O; the bands at 3625 and 3695 cm^{-1} correspond to OH groups of halloysite-10 Å. No

TABLE 4. Crystal data, data-collection information and refinement details.

Space group	*Pnma* (#62)
Cell parameters	
a (Å)	6.38270(12)
b (Å)	6.86727(12)
c (Å)	4.39168(8)
V (Å^3)	192.495(6)
Z	4
Structural formula	$(Y_{0.832}\ Dy_{0.168})F_3$
$D_{calc.}$ (g/cm^3)	5.543
μ (mm^{-1})	74.130
Data collection	
Diffractometer	Rigaku R-AXIS RAPID II
Radiation	Cu*K*α (graphite-monochromatized)
Temperature	298 K
Crystal size (mm)	0.05 × 0.03 × 0.02
$2\theta_{max.}$	136.4º
Total no. oscillation images	180
Fundamental sweeps ω (º)	80.0−260.0 in 5.0 steps
χ (º)	54.0
φ (º)	0, 90, 180, 270
exposure rate (s/º)	60
Another sweep ω (º)	80.0− 60.0 in 5.0 steps
χ (º)	0
φ (º)	0
exposure rate (s/º)	60
Index ranges	$-7 \leqslant h \leqslant 7$; $-8 \leqslant k \leqslant 8$; $-5 \leqslant l \leqslant 5$
Total no. reflections	1941
No. unique reflections	193
No. reflections, $I > 2\sigma(I)$	191
$R_{int.}$	0.0360
Refinement	
No. of variable parameters	24
*R*1, $I > 2\sigma(I)$	0.0163
*R*1, all data	0.0173
w*R*2, all data	0.0388
Goof	1.041
$\Delta\rho_{min.}$, $\Delta\rho_{max.}$ (e / Å^3)	−0.596, 0.532

$R1 = \Sigma||F_o| - |F_c|\ | / \Sigma|F_o|$; $wR2 = \{\Sigma[w(F_o^2 - F_c^2)^2] / \Sigma\ [w(F_o^2)^2]\}^{0.5}$; $w = 1/[\sigma^2(F_o^2) + (aP)^2 + bP]$; $P = [2\ F_c^2 + F_o^2]/3$

https://doi.org/10.1180/minmag.2015.079.3.18 Published online by Cambridge University Press

other bands of OH groups are observed in the IR spectrum. Halloysite is poorly crystallized (which is typical of this mineral) and could not be detected by XRD. However, multiple distinct bands present in the IR spectrum definitely indicate its presence. The IR spectrum demonstrates the absence of carbonate and borate groups.

Crystallography

Powder XRD data for waimirite-(Y) from Brazil were obtained with a D8 Advance DaVinci diffractometer using Cu$K\alpha$ radiation at the X-ray Diffraction Laboratory, Geosciences Institute, University of São Paulo. Data (in Å for Cu$K\alpha$) are given in Table 3. Unit-cell parameters refined from powder data (indexed by analogy with the synthetic equivalent) are as follows: Orthorhombic, *Pnma*, a = 6.386(1), b = 6.877(1), c = 4.401(1) Å, V = 193.28(7) Å^3, Z = 4, $a:b:c$ = 0.929:1:0.640.

The XRD investigations of waimirite-(Y) from Saudi Arabia were carried out with a single-crystal fragment of small size (0.05 mm × 0.03 mm × 0.02 mm) that was picked from the thin section used for the electron-microprobe analysis. The powder XRD pattern was obtained using a Gandolfi camera, 114.6 mm in diameter, employing Ni-filtered Cu$K\alpha$ radiation. The data were recorded on an imaging plate and processed with a Fuji BAS-2500 bio-image analyser using a computer program written by Nakamuta (1999). The XRD pattern (Table 3) is basically identical to those of waimirite from the type locality and of the synthetic YF_3 (Greis, 1976). The unit-cell parameters were refined with an internal Si-standard reference material (NBS #640b) using a computer program by Toraya (1993); a = 6.381(2), b = 6.870(2), c = 4.3915(12) Å, V = 192.51(10) Å^3, Z = 4, which are comparable to those refined from the single-crystal X-ray diffraction (SCXRD) data a = 6.38270(12), b = 6.86727(12), c = 4.39168(8) Å, V = 192.495(6) Å^3, Z = 4.

The SCXRD data were obtained from the same fragment on a Rigaku R-AXIS RAPID curved imaging plate diffractometer using Cu$K\alpha$ radiation monochromatized and focused by a VariMax confocal multilayer mirror. The orthorhombic space group symmetry of *Pnma* was suggested by extinctions in the SCXRD data. Experimental details of the data collection are given in Table 4. The data were corrected for absorption, empirically, Lorentz and polarization effects. The positions of Y and F atoms in the synthesized YF_3, determined by Cheetham and Norman (1974), were used as starting parameters in the present refinement of *SHELXL-97* (Sheldrick, 2008). The scattering factors for the neutral atoms and anomalous dispersion factors were taken from the *International Tables for X-ray Crystallography, Volume C* (Wilson, 1992). As Dy is the predominant lanthanide in waimirite-(Y) from Saudi Arabia, the scattering curve of Dy was employed in the calculations representing the lanthanides (*Ln*). The occupancy parameters of Y and Dy were refined at the Y site. The refinement converged into R_1 = 0.0163 and wR_2 = 0.0388 for 191 reflections with $F_o > 2\sigma(F_o)$. The final positional parameters, the equivalent isotropic

TABLE 5. Final atom positions, equivalent and anisotropic displacement parameters (Å^2) for waimirite-(Y) from Saudi Arabia.

Site	x/a	y/b	z/c	U_{eq}		
Y*	0.36773(6)	0.25	0.44001(10)	0.0033(3)		
F1	0.0234(5)	0.25	0.5896(8)	0.0093(9)		
F2	0.1649(4)	0.0635(4)	0.1220(6)	0.0086(8)		
Site	U^{11}	U^{22}	U^{33}	U^{23}	U^{13}	U^{12}
Y*	0.0037(3)	0.0011(3)	0.0049(4)	0	−0.00086(15)	0
F1	0.0096(18)	0.0088(18)	0.0095(17)	0	0.0010(13)	0
F2	0.0093(12)	0.0061(14)	0.0103(12)	−0.0015(10)	−0.0004(10)	−0.0001(9)

* 0.832(18)Y + 0.168Dy.

https://doi.org/10.1180/minmag.2015.079.3.18 Published online by Cambridge University Press

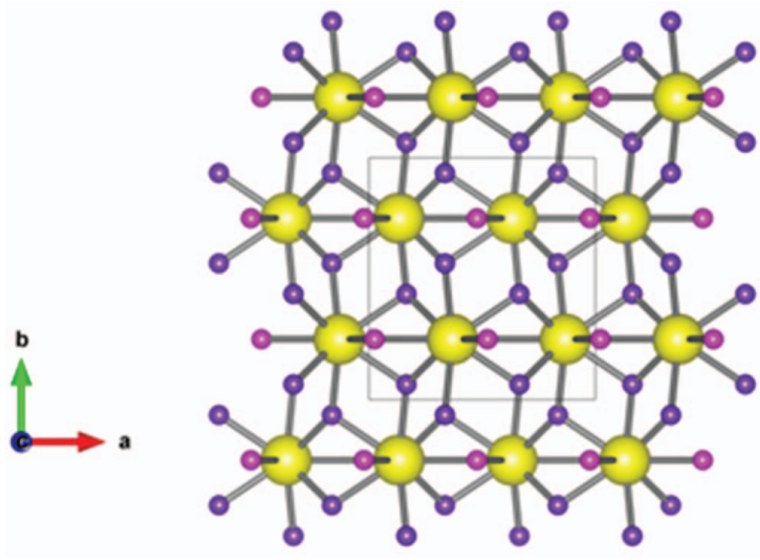

FIG. 5. A projection of the crystal structure of waimirite-(Y) onto (001) drawn using *VESTA* (Momma and Izumi, 2011). Yellow, pink and purple spheres indicate Y, F1 and F2, respectively.

displacement parameters and the anisotropic displacement parameters are given in Table 5. The crystal structure of waimirite-(Y) drawn using *VESTA* (Momma and Izumi, 2011) is shown in Fig. 5. Selected interatomic distances are summarized in Table 6. The bond valences were calculated from the interatomic distances following the procedure of Brown and Altermatt (1985), using the parameters of Brese and O'Keeffe (1991) and are listed in Table 7.

Discussion

Two polymorphs are known for YF_3, the trigonal ($P\bar{3}c1$, #165) (Uvarov *et al.*, 1984) having the fluocerite-type structure (Garashina *et al.*, 1980) and the orthorhombic (*Pnma*, #62) (Zalkin and Templeton, 1953; Cheetham and Norman, 1974). Trifluorides of rare-earth elements (*REE*: Y and lanthanoids, *Ln*, La–Lu) crystallize in the orthorhombic structure for Y, and *Ln* as small as Y, namely Sm–Lu, only, whereas trigonal LnF_3 has

TABLE 6. Interatomic distances (Å) for waimirite-(Y) from Saudi Arabia and isostructural synthetic analogues.

Waimirite-(Y) (Saudi Arabia)*		YF_3**	SmF_3***	HoF_3**	YbF_3**
Y–F1	2.292(3)	2.282(4)	2.37	2.30	2.22
–F1	2.294(3)	2.287(4)	2.39	2.32	2.25
–F2 ×2	2.295(2)	2.281(3)	2.36	2.28	2.27
–F2 ×2	2.305(2)	2.299(3)	2.37	2.31	2.27
–F2 ×2	2.306(2)	2.310(2)	2.39	2.31	2.27
–F1	2.529(3)	2.538(4)	2.49	2.50	2.61
Mean	2.325	2.321	2.39	2.32	2.30
a (Å)	6.38270(12)	6.3537(7)	6.676	6.410	6.218
b (Å)	6.86727(12)	6.8545(7)	7.062	6.873	6.785
c (Å)	4.39168(8)	4.3953(5)	4.411	4.376	4.431
V (Å^3)	192.495(6)	191.42	207.96	192.79	186.94

* Present study; ** Cheetham and Norman (1974); *** Bukvetskii and Garashina (1977).

https://doi.org/10.1180/minmag.2015.079.3.18 Published online by Cambridge University Press

TABLE 7. Bond-valence sums weighted on the occupancies for waimirite-(Y) from Saudi Arabia.

	—— Y ($Y_{0.832}Dy_{0.168}$) ——			Sum
F1	0.353	0.351	0.186	0.891
	0.351			
	0.186			
F2	0.350	0.341	0.340	1.032
	0.350	0.341	0.340	1.032
	0.341			
	0.341			
	0.340			
	0.340			
Sum	2.955			2.955

been reported for all *REE* with any size of ions. The trigonal *REE*F_3 minerals are rich in the larger *Ln* ions, i.e. *LREE*, and are known and described as dominated by Ce or La, fluocerite-(Ce) (Styles and Young, 1983) and fluocerite-(La) (Chistyakova and Kazakova, 1969), respectively. In the crystal structure of fluoceite-(Ce) and its synthetic *Ln*-equivalents, *REE* are coordinated by nine F atoms with two more distant neighbours (Zalkin and Templeton, 1985; Kondratyuk *et al*., 1988).

On the other hand, waimirite-(Y), YF_3, is the only *REE*F_3 orthorhombic mineral species. The Y atom forms a 9-coordinated YF_9 tricapped trigonal (an YF_6 trigonal prism with an extra F atom attached to each of its three rectangular faces) in the crystal structure of orthorhombic YF_3 (Cheetham and Norman, 1974). The present crystallographic investigation confirmed that the crystal structure of waimirite-(Y) is isostructural with the synthetic orthorhombic YF_3, as well as the *Ln*F_3 (Bukvetskii and Garashina, 1977 for Sm, Ho and Yb; Garashina and Vishnyakov, 1977 for Ho).

The unit-cell volume of orthorhombic *REE*F_3 (*REE* = Y and Sm–Lu) tends to increase with increasing ionic radii of REE^{3+}. However, as Garashina *et al*. (1980) pointed out, the increase is not isotropic. One dimension, *c*, remains mostly constant and decreases slightly with the increase in the radii of REE^{3+}, whereas two other dimensions, *a* and *b*, increase. Garashina *et al*. (1980) explained the anisotropy in the unit cell with the anomalous *REE*–F interatomic distance. The longest distance among nine *REE*–F of the *REE*O_9 polyhedron decreases, although the other shorter eight *REE*–F distances increase, as usual, with increasing ionic radii of REE^{3+}. Garashina *et al*. (1980) suggested a reduction in the contribution of the 9th F for the chemical bond to *REE*. Such structural features relating to the REE^{3+} radius were observed in waimirite-(Y) from Saudi Arabia. The *REE*–F interatomic distances and unit-cell parameters of waimirite-(Y) are close to those of synthetic YF_3 and HoF_3 (Table 6). The bond-valence calculation (Table 7) revealed the scarce contribution in chemical bond between the 9th F and (Y,Dy) [0.186] in waimirite-(Y) from Saudi Arabia.

About 80 atomic % of *REE*s are Y in waimirite-(Y) from Saudi Arabia and the remaining 20% are lanthanoids (La–Lu). Dysprosium is the dominant element among the lanthanoids. The chemistry of waimirite-(Y) from Saudi Arabia shows a lanthanoid distribution pattern rich in *HREE* (Fig. 6). The replacement of *HREE* such as Dy

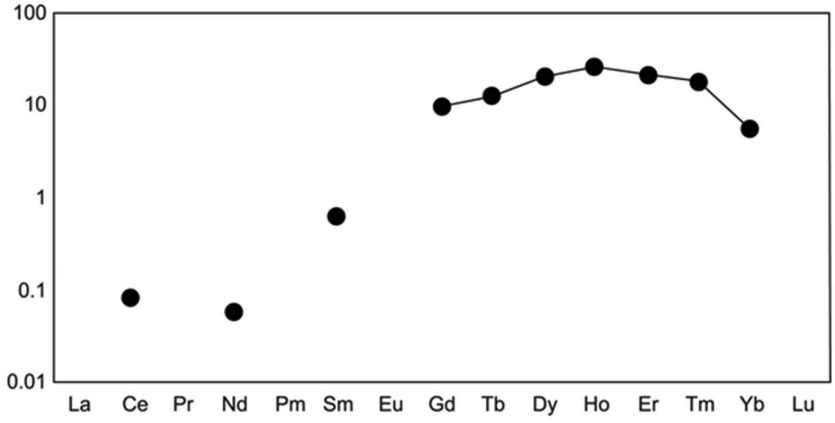

FIG. 6. Chondrite-normalized lanthanide distribution pattern of waimirite-(Y).

https://doi.org/10.1180/minmag.2015.079.3.18 Published online by Cambridge University Press

for Y conduce very slight variation in crystallographic values of waimirite-(Y) from Saudi Arabia in comparison to the pure YF_3. Consequently, the unit-cell parameters and interatomic distances of waimirite-(Y) from Saudi Arabia are very close to those of pure YF_3. Dysprosium has been a valued resource for recent material engineering in magnet industries. Waimirite-(Y), $(Y,Dy)F_3$, is the most important ore mineral in the *REE* deposit at Jabal Tawlah, Saudi Arabia.

Acknowledgements

The authors acknowledge the Brazilian agencies FAPESP (processes 2011/22407-0 and 2013/03487-8), CNPq (process 485415/12-7) and FINEP for financial support, all members of the IMA-CNMNC, the Principal Editor, Peter Williams, and the reviewers Ian Grey, Ian Graham and an anonymous reviewer for their helpful suggestions and comments.

References

Bastos Neto, A.C., Pereira, V.P., Ronchi, L.H., Lima, E.F. and Frantz, J.L. (2009) The world-class Sn-Nb-Ta-F(Y, *REE*, Li) deposit and the massive cryolite associated with the albite-enriched facies of the Madeira A-type granite, Pitinga mining district, Amazonas State, Brazil. *The Canadian Mineralogist*, **47**, 1329–1357.

Bastos Neto, A.C., Pereira, V.P., Pires, A.C., Barbanson, L. and Chauvet, A. (2013) Fluorine-rich xenotime from the Madeira world-class Nb-Ta-Sn deposit associated with the albite-enriched granite at Pitinga, Amazonia, Brazil. *The Canadian Mineralogist*, **50**, 1453–1466.

Bastos Neto, A.C., Ferron, J.T.M.M., Chauvet, A., Chemale, F., Lima, E.F., Barbanson, L. and Costa, C.F.M. (2014*a*) U-Pb dating of the Madeira Suite and structural control of the albite-enriched granite at Pitinga (Amazonia, Brazil): Evolution of the A-type magmatism and implications for the genesis of the Madeira Sn-Ta-Nb (*REE*, cryolite) world-class deposit. *Precambrian Research*, **243**, 181–196.

Bastos Neto, A.C., Pereira, V.P., Atencio, D., Ferron, J.T.M.M. and Coutinho, J. (2014*b*) Waimirite-(Y), IMA 2013-108. CNMNC, Newsletter 19, February 2014, pages 167–168. *Mineralogical Magazine*, **78**, 165–170.

Brese, N.E. and O'Keeffe, M. (1991) Bond-valence parameters for solids. *Acta Crystallographica*, **B47**, 192–197.

Brown, I.D. and Altermatt, D. (1985) Bond-valence parameters obtained from a systematic analysis of the Inorganic Crystal Structure Database. *Acta Crystallographica*, **B41**, 244–247.

Bukvetskii, B.V. and Garashina, L.S. (1977) Crystal-chemical investigation of the orthorhombic trifluorides of samarium, holmium, and ytterbium. *Coordination Chemistry*, **3**, 791–795 [translated from *Koordinatsionnaya Khimiya*, **3**, 1024–1029].

Cheetham, A.K. and Norman, N. (1974) The structures of yttrium and bismuth trifluorides by neutron diffraction. *Acta Chemica Scandinavica*, **A28**, 55–60.

Cheetham, A.K., Fender, B.E.F., Fuess, H. and Wright, A.F. (1976) A powder neutron diffraction study of lanthanum and cerium trifluorides. *Acta Crystallographica*, **B32**, 94–97.

Chistyakova, M.B. and Kazakova, M.E. (1969) Fluocerite from Kazakhstan. *Trudy Mineralogicheskogo Muzeya Akademiya Nauk SSSR*, **19**, 236–238 [in Russian].

Chukanov, N.V (2014) *Infrared Spectra of Mineral Species: Extended Library*. Springer-Verlag GmbH, Dordrecht–Heidelberg–New York–London, pp. 1716.

Garashina, L.S. and Vishnyakov, Yu.S. (1977) Structural changes in the series $LnFeO_3$ and LnF_3. *Soviet Physics Crystallography*, **22**, 313–315 [translated from *Kristallografiya*, **22**, 547–555].

Garashina, L.S., Sobolev, B.P., Aleksandrov, V.B. and Vishnyakov, Y.S. (1980) Crystal chemistry of rare earth fluorides. *Soviet Physics Crystallography*, **25**, 171–174.

Greis, O. (1976) *Preparative, strukturelle und thermochemische Untersuchungen an Selten-Erd-Fluoriden under bedsonderer Berucksichtigung der Elemente Samarium, Europium, Thulium und Ytterbium*. Inaugural-Dissertation, Albert-Ludwigs-Universitat, Freiburg, Germany, pp. 330.

Kollia, Z., Sarantopoulou, E., Cefalas, A.C., Nicolaides, C.A., Naumov, A.K., Semashko, V.V., Abdulsabirov, R.Y., Korableva, S.L. and Dubinskii, M.A. (1995) Vacuum-ultraviolet interconfigurational $4f3 \rightarrow 4f25d$ absorption and emission studies of the Nd^{3+} ion in KYF, YF, and YLF crystal hosts. *Journal of the Optical Society of America B*, **12**, 782–785.

Kondratyuk, I.P., Loshmanov, A.A., Muradyan, L.A., Maksimov, B.A., Sirota, M.I., Krivandina, E.A. and Sobolev, B.P. (1988) Neutron-diffraction study on NdF_3. *Soviet Physics, Crystallography*, **33**, 57–60.

Lage, M.M., Righi, A., Matinaga, F.M., Gesland, J.-Y. and Moreira, R.L. (2004) Raman-spectroscopic study of lanthanide trifluorides with the β-YF_3 structure. *Journal of Physics: Condensed Matter*, **16**, 3207–3218.

Minuzzi, O.R.R., Ferron, J.M.T.M., Bastos Neto, A.C. and Pereira, V.P. (2003) Primeira notícia da

https://doi.org/10.1180/minmag.2015.079.3.18 Published online by Cambridge University Press

descoberta de waimirita e atroarita, dois novos minerais na Mina de Pitinga, AM, Brasil. *Pesquisas em Geociências*, **30**, 99–101.

Momma, K. and Izumi, F. (2011) VESTA 3 for three-dimensional visualization of crystal, volumetric and morphology data. *Journal of Applied Crystallography*, **44**, 1272–1276.

Nakamuta, Y. (1999) Precise analysis of a very small mineral by an X-ray diffraction method. *Journal of the Mineralogical Society of Japan*, **28**, 117–121 [in Japanese with English abstract].

Nowacki, W (1938) Die Kristallstruktur des kubischen Yttriumfluorids YF_3. *Zeitschrift für Kristallographie*, **100**, 242–250.

Qian, L.W., Zai, J.T., Chen, Z., Zhu, J., Yuan, Y.P. and Qian, X.F. (2010) Control of the morphology and composition of yttrium fluoride via a salt-assisted hydrothermal method. *CrystEngComm*, **12**, 99–206.

Rotereau, K., Gesland, J.Y., Daniel, P. and Bulou, A. (1993) Raman scattering study of Czochralski-grown yttrium fluoride single crystals. *Materials Research Bulletin*, **28**, 813–819.

Sheldrick, G.M. (2008) A short history of SHELX. *Acta Crystallographica*, **A64**, 112–122.

Sorokin, N.I., Sobolev, B.P. and Breiter, M.W. (2002) Specific features of anion transfer in HoF_3 crystals at high temperatures. *Physics of the Solid State*, **44**, 282–285.

Styles, M.T. and Young, B.R (1983) Fluocerite and its alteration products from the Afu Hills, Nigeria. *Mineralogical Magazine*, **47**, 41–46.

Toraya, H. (1993) The determination of unit-cell parameters from Bragg reflection data using a standard reference material but without a calibration curve. *Journal of Applied Crystallography*, **26**, 585–590.

Trnovcová, V., Garashina, L.S., Škubla, A., Fedorov, P.P., Čička, R., Krivandina, E.A. and Sobolev, B.P. (2003) Structural aspects of fast ionic conductivity of rare earth fluorides. *Solid State Ionics*, **157**, 195–201.

Uvarov, N.F., Hairetdinov, E.F. and Boldyrev, V.V. (1984) Correlations between parameters of melting and conductivity of solid lonic compounds. *Journal of Solid State Chemistry*, **51**, 59–68.

Watanabe, Y., Hoshino, M. and Moriyama, T. (2014) Jabal Tawlah, a heavy *REE*-rich prospect in north-west Saudi Arabia. *21st General Meeting of the International Mineralogical Association, Johannesburg, South Africa*, Abstract p. 62.

Wilson, A.J.C. (editor) (1992) *International Tables for Crystallography, Volume C*. Kluwer Academic Publishers, Dordrecht, The Netherlands, 883 pp.

Zalkin, A. and Templeton, D.H. (1953) The crystal structures of YF_3 and related compounds. *Journal of the American Chemical Society*, **75**, 2453–2458.

Zalkin, A. and Templeton, D.H. (1985) Refinement of the trigonal crystal structure of lanthanum trifluoride with neutron diffraction data (fluocerite). *Acta Crystallographica*, **B41**, 91–93.

https://doi.org/10.1180/minmag.2015.079.3.18 Published online by Cambridge University Press